

Supporting Information

**Design of well-defined shape memory networks with high
homogeneity: towards advanced shape memory polymeric materials**

*Xingjian Li, Yi Pan, Jingjuan Lai, Ruiqing Wu, Zhaohui Zheng, and Xiaobin Ding**

CONTENTS:

Section S1. Fabrication of PDLLA-4NB.

Section S2. Determining C^* of the PDLLA-4NB.

Section S3. Fabrication of SM-PN.

Section S4. Fabrication of CP-SMP.

Section S5. Thermomechanical Properties.

Section S6. Shape memory performance.

Section S7. Stress relaxation isothermal tests.

Section S8. The multi-shape memory testing.

Section S9. Multi-SME of semi-IPNs:

Section S1. Fabrication of PDLLA-4NB:

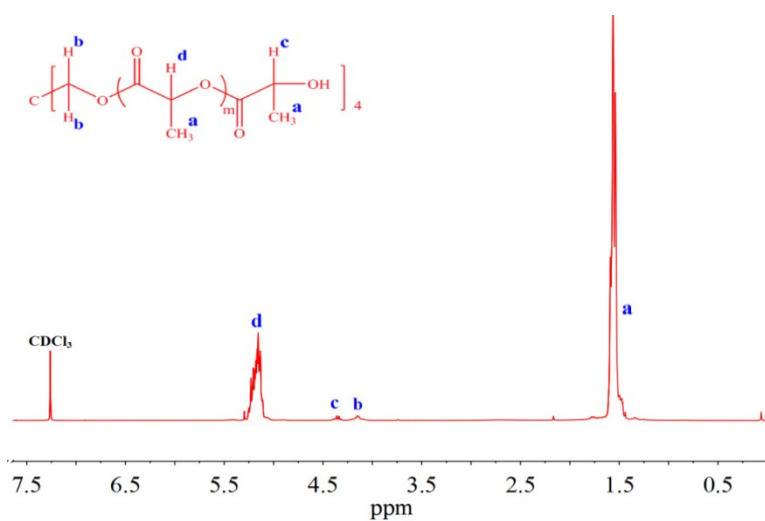


Figure S1. ¹H NMR (300 MHz, CDCl₃) of the as-prepared four-arm PDLLA. The PET hydroxyl protons are completely reacted to form 4-arm star-shaped molecules based on the signal of PET methylene protons

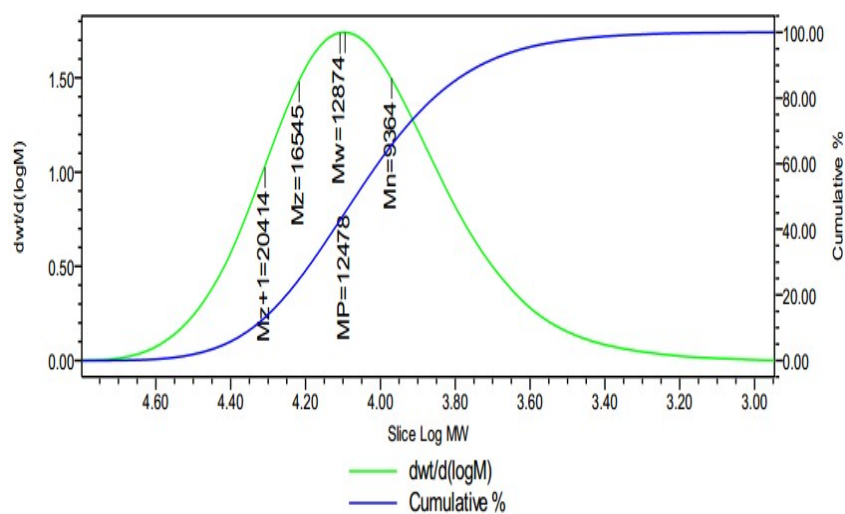


Figure S2. GPC of the as-prepared four-arm PDLLA macromer. The theoretical number-averaged molecular weights (M_n) of PDLLAs were approximately 10936 g/mol, which were very similar to the M_n (9364 g/mol) with polydispersity index close to 1.37 obtained by GPC.

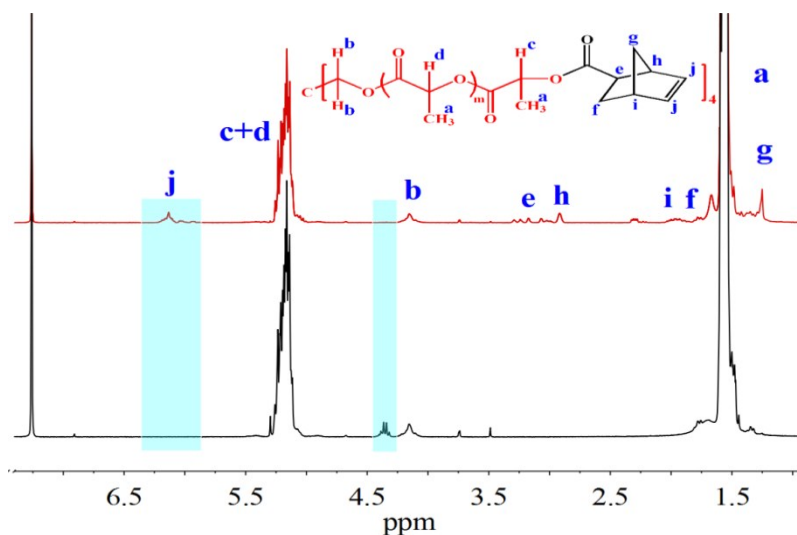


Figure S3. ^1H NMR (300 MHz, CDCl_3) of the PDLLA-4NB and four-arm PDLLA. PDLLA-4NB had an end group conversion of 100%.

Section S2. Determining C^* of the PDLLA-4NB:

The relative viscosity of norbornene-functionalized four-arm PDLLA chloroform solution was measured with a Physica MCR 301 (Anton Paar, Austria) rotational rheometer equipped with a Searle-type concentric cylinder geometry CC27 (ISO3219). Samples were equilibrated at the temperature of interest for no less than 10 min prior to the measurements. All experiments were carried out at 25 °C. At a constant shear rate of 100 s^{-1} , the shear duration of each measuring is 300 s for concentrations between 4 and 100 mg/ml. In order to determining C^* of the PDLLA-4NB, its relative viscosity measured by a rheometer as a function of the polymer concentration is plotted (**Figure S4**). C^* of the PDLLA-4NB was estimated to 63.6 mg/mL (**Figure S5**).

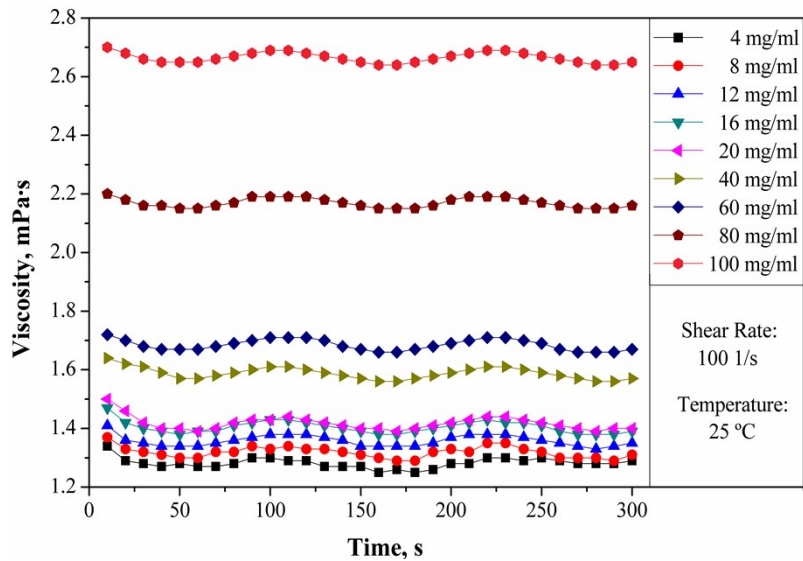


Figure S4. The shear viscosity of norbornene-functionalized 4-arm poly(D, L-lactide) as a function of polymer concentration.

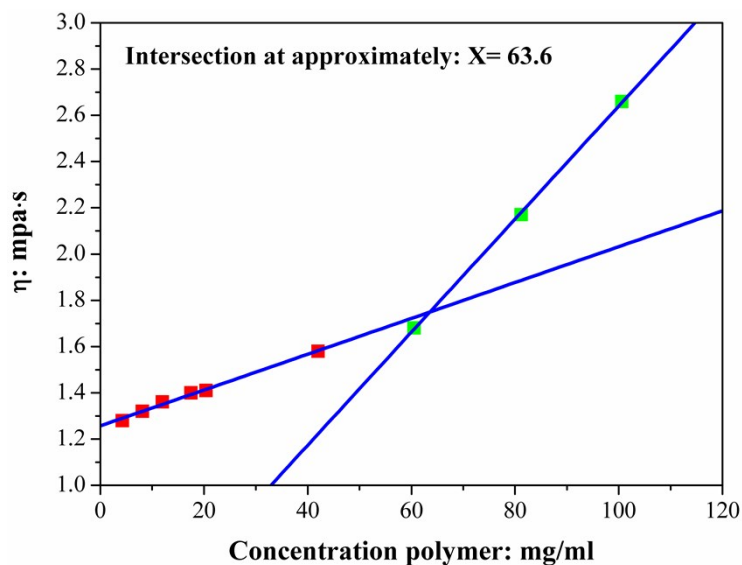


Figure S5. The determination of C^* for norbornene-functionalized 4-arm poly(D, L-lactide).

Section S3. Fabrication of SM-PN:

In glass mold, the gelation behavior also was examined under different light intensities (**Figure S6**). Initiation at even far below 10 mW/cm^2 light intensity on the mold surface results in gelation of the mixture within 20 minutes. To ensure a high gel fraction, all samples were prepared in about 10 mW/cm^2 light intensity for 1 h.

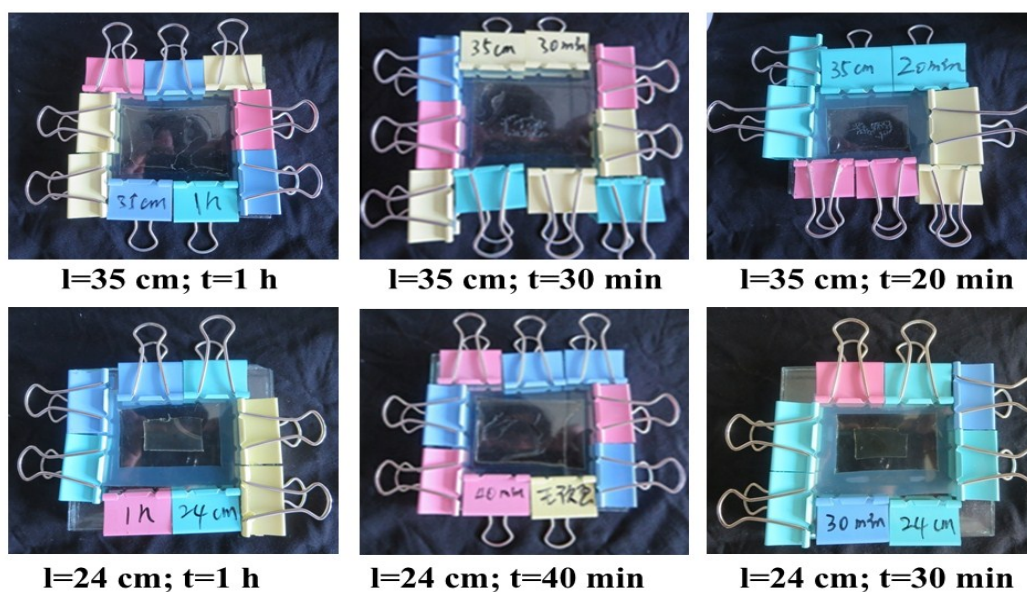


Figure S6. Gel behavior of the reaction system under different light intensity (l : between the mold and the UV lamp) and time (t). (When the mold is at 20 cm from the UV lamp, the light intensity of the glass (thickness is 5 mm) surface is approximately 10 mW cm^{-2})

Section S4. Fabrication of CP-SMP:

The four-arm PDLA (25 g, 2.675 mmol) was dissolved in freshly distilled dichloromethane (175 ml) under a nitrogen atmosphere. Upon cooling in an ice bath, dry triethylamine (2.7 g, 26.75 mmol) and acryloyl chloride (2.42 g, 26.75 mmol) were added dropwise and the mixture was stirred for 3 days at room temperature. The precipitated ammonium salt was separated by filtration. The concentrated filtrate was precipitated in a tenfold excess of cold methanol. The precipitation purification was repeated 3 times. The product was dried under vacuum. PDLA-4DA had an end group conversion of 100% by $^1\text{H NMR}$ (**Figure S7**).

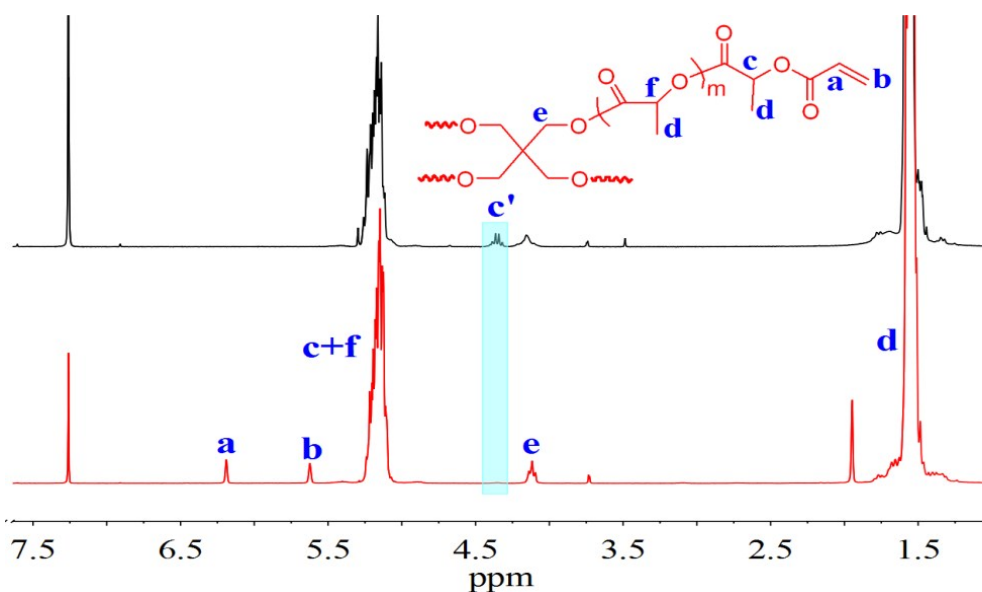


Figure S7. ^1H NMR (300 MHz, CDCl_3) of the PDLLA-4DA and four-arm PDLLA.

The preparation of PDLLA-4DA and CP-SMP was shown in **Figure S8**. PDLLA-4DA (5.00 g) was dissolved in chloroform (10 mL) along with the initiator DMAP (0.50 wt% relative to PDLLA-4DA). A homogeneous solution was obtained by an eddy mixer. The solution was injected to a custom-made glass mold that consisted of two silanized glass slides with a 1 mm thick silicone rubber spacer placed in between the glass slides ($8 \times 6.5 \times 0.1 \text{ cm}^3$). The mixture was exposed to a UV light source with 10 mW/cm^2 light intensity in a custom-made UV curing box for 20 min. The cured samples (CP-SMP) were removed from the mold and then placed at room temperature for 48 h. The samples were dried in vacuum oven at $60 \text{ }^\circ\text{C}$ for 24 h and then at $80 \text{ }^\circ\text{C}$ for 12 h.

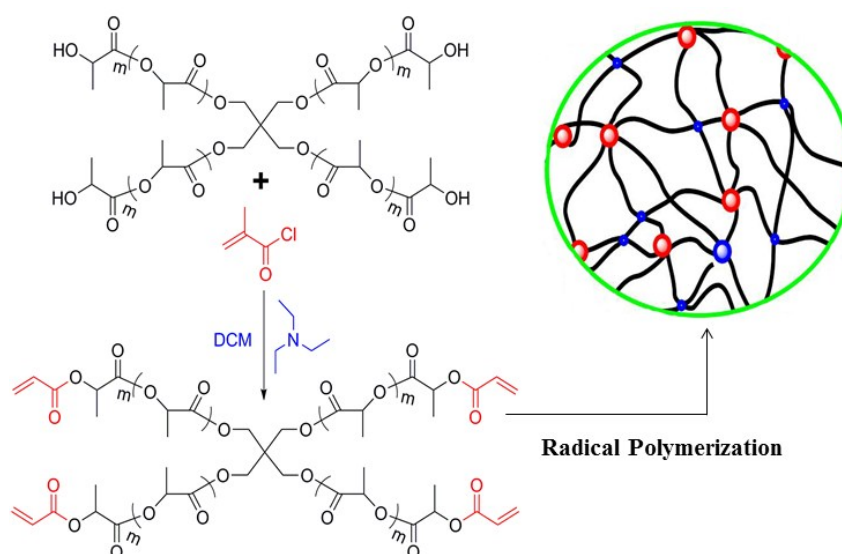


Figure S8. The preparation of PDLLA-4DA and CP-SMP (red circles are multifunctional cross-links from radical polymerization of acrylate end-groups; blue circles denote tetra-functional cross-links originating from the prepolymer.)

Section S5. Thermomechanical Properties:

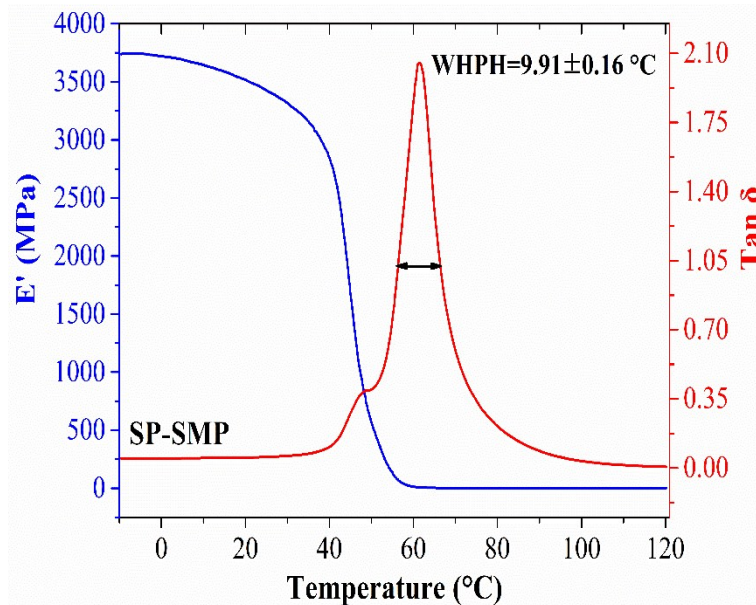


Figure S9. Evolution of the storage modulus (E') and loss angle ($\tan \delta$) as a function of temperature (at frequency 1 Hz) for SM-PN.

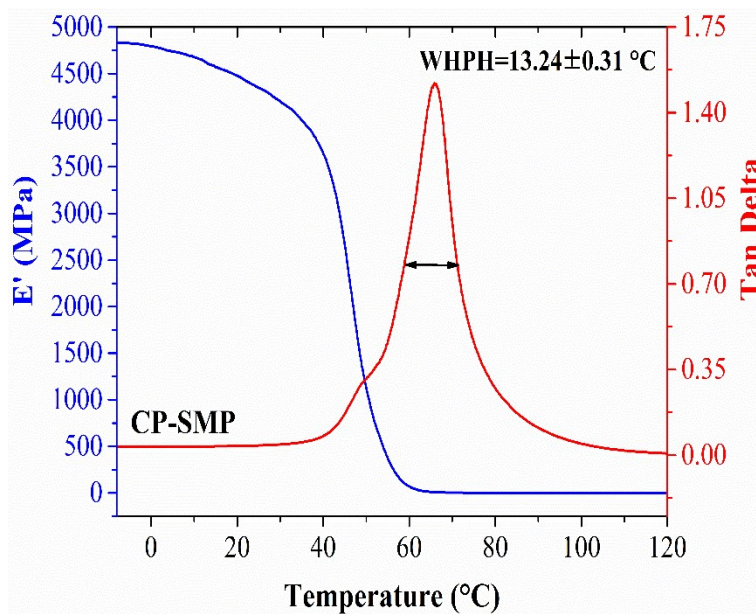


Figure S10. Evolution of the storage modulus (E') and loss angle ($\tan \delta$) as a function of temperature (at frequency 1 Hz) for CP-SMP.

Table S1. The crosslinking strategy, WHPH and reference of various SMPs.

No.	Polymer systems	Cross-linking Strategies	WHPH (°C)	Ref.
Cross-linked poly(lactide) homopolymer or copolymer networks (A)				
[1]	SM-PN	thiol-norbornene	9.9	In this work
[2]	CP-SMP	radical-chain-growth polymerization	12.9	In this work
[3]	POSS-PLA	hydroxy-isocyanate	8.7~9.4	1
[4]	oligo[(L-lactide)-ran-glycolide]dimethacrylates	radical-chain-growth polymerization	13.9	2
[5]	POSS-PLGA	thiol-ene	14.1	3
[6]	PR4t10tN	radical-chain-growth polymerization	27.5	4
[7]	PR4t8tN	radical-chain-growth polymerization	37.5	4
Thiol-X (X = norbornene, epoxy, maleimide, isocyanate and ene) polymer systems (B)				
[8]	3T/DA	thiol-ene	8.5	5
[9]	4T/DA	thiol-ene	9.0	5
[10]	thiol-epoxy polymers	thiol-ppoxy	10.3-15.7	6
[11]	ternary thiol-thiol-ene systems	thiol-ene	12-17	7
[12]	TMICN/BPADGE	thiol-epoxy	23.8	8
[13]	4T/BMI	thiol-maleimide	24.0	5
[14]	3T/BMI	thiol-maleimide	26.0	5
[15]	PETMP/HMDI/IEM	thiol-isocyanate	26.3	9
[16]	step-growth thiol-ene systems	step-growth thiol-ene	12-30	10
[17]	ester-free thiol-X resins	thiol-michael and thiol-ene	20-30	11
[18]	Thiol-norbornene material	thiol-norbornene	9-38	12
[19]	UPyA/PEGDA/PTME	step-growth thiol-ene reaction	67.2	13
Copper(I)-catalyzed azide-alkyne cycloaddition and double click aza-Michael addition polymer systems (C)				
[20]	PETMP tetra-yne and BPAdiazide	copper(I)-catalyzed azide-alkyne cycloaddition	15	14.
[21]	poly(amino ester)-poly(acrylate)s	double click aza-Michael addition and radical polymerization.	15.2	15
[22]	phenolic cross-linked epoxy resin	copper catalyzed azide-alkyne cycloaddition	28.8	16
[23]	tris(4-(1-azido 3-oxy propan-2-ol)phenyl) methane and propargyl functionalized novolac oligomer	copper catalyzed azide-alkyne cycloaddition	39.9	17
[24]	propargylated bisphenol-F and a tris azide	copper catalyzed azide-alkyne cycloaddition	57.6	18
AB copolymer networks (D)				
[25]	PDMAEt	radical-chain-growth polymerization	16.5-22.3	19
[26]	BA-co-PEGDMA		18.3-22.8	20
[27]	M/E/P-co- BAE		19-23	21
[28]	tBA/PEGDMA		24	10
[29]	MMA-co-PEGDMA		22.5-26.3	22
[30]	M/E/P-co- BA		23-32	21
[31]	PDMABu		22.8-82.8	19

Semi-interpenetrating polymer networks (E)				
[32]	PMMA/PEG	radical-chain-growth polymerization	28-32	23
[33]	IPN-6 wt%		29.5	24
[34]	IPN-4 wt%		34.7	24
[35]	P(MMA-co-VP)/PEG		31	25
[36]	PMMA/SPEG (A1)		33	26
[37]	PMMA/SPEG (A2)		42	26
[38]	PMMA/SPEG (A3)		55	26
[39]	PMMA/SPEG (A4)		54	26
[40]	PMMA-PEG2000 semi-IPN		38.5	27
Some other polymer systems (F)				
[41]	zwitterionic polyurethanes	–	26.7-34.4	28
[42]	MMA-co-PEGDMA	radical-chain-growth polymerization	34-38	29
[43]	perfluorosulphonic acid ionomer	–	41.3	30
[44]	poly(benzoxazole-co-imide)s	–	41.1-50.8	31

Section S6. Shape memory performance:

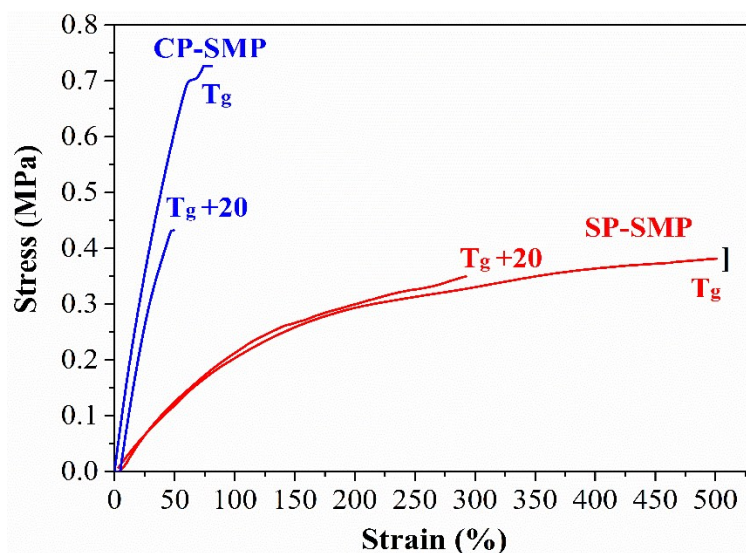


Figure S11. Typical uniaxial stress–strain curves at different temperatures (T_g and $T_g + 20$) for CP-SMP and SM-PN.

Table S2 Measured SME parameters of the SM-PN sample for six cycles.

Cycle	$\varepsilon_n(\%)$	$\varepsilon_m(\%)$	$\varepsilon_u(\%)$	$\varepsilon_p(\%)$	$R_f(\%)$	$R_r(\%)$
1st	3.89	70.30	70.30	4.28	100.0	99.4
2nd	4.28	102.3	102.2	5.63	99.9	98.6
3rd	5.63	182.1	181.9	7.01	99.9	99.2
4th	7.01	237.6	237.4	16.25	99.9	96.0
5th	16.25	291.6	291.3	31.53	99.9	94.4
6th	31.53	431.6	431.3	69.97	99.9	90.4

Table S3 Measured SME parameters of the SM-PN sample repeated for fifteen cycles at the strain above 100%.

Cycle	$\varepsilon_n(\%)$	$\varepsilon_m(\%)$	$\varepsilon_u(\%)$	$\varepsilon_p(\%)$	$R_f(\%)$	$R_r(\%)$	$V_r(\%/^{\circ}\text{C})$
1st	1.506	109.5	109.4	10.18	99.91	91.96	25.48
2nd	10.18	112.5	112.3	10.91	99.80	99.29	23.88
3rd	10.91	112.8	112.7	11.17	99.90	99.74	24.69
4th	11.17	112.7	112.6	11.26	99.90	99.91	26.06
5th	11.26	113.1	113.0	11.41	99.90	99.85	26.06
6th	11.41	112.8	112.6	11.48	99.80	99.93	27.68
7th	11.48	113.0	112.8	11.65	99.80	99.83	27.59
8th	11.65	112.6	112.5	11.68	99.90	99.97	27.97
9th	11.68	112.7	112.5	11.80	99.80	99.88	28.07
10th	11.80	112.4	112.3	11.80	99.90	100.0	28.88
11th	11.80	112.8	112.7	11.98	99.90	99.82	27.12
12th	11.98	112.6	112.5	12.00	99.90	99.98	27.21
13th	12.00	113.0	112.9	12.14	99.90	99.86	27.59
14th	12.14	112.7	112.5	12.15	99.80	99.99	27.87
15th	12.15	112.7	112.6	12.23	99.90	99.92	27.97

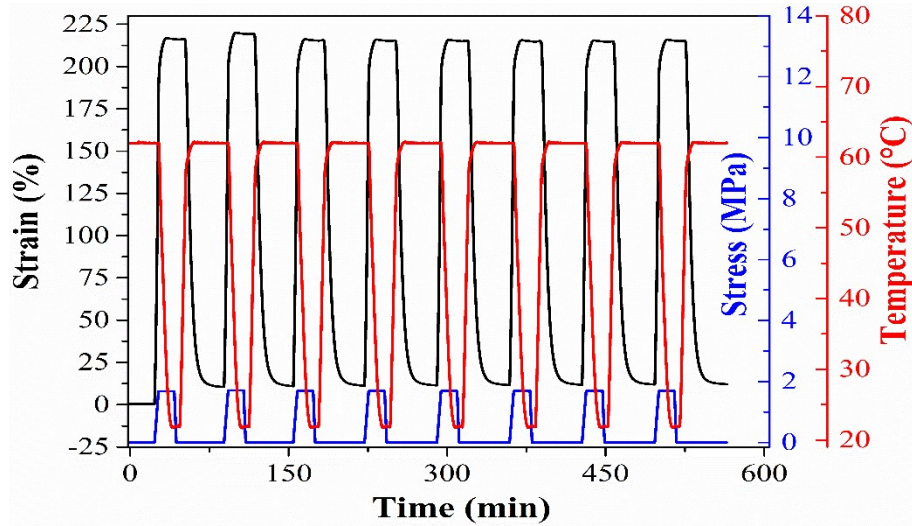


Figure S12. Consecutive shape memory cycles for SM-PN at the strain above 200% (b) at $T_d = T_r = T_g$ and $T_f = T_g - 40$.

Table S4 Measured SME parameters of the SM-PN sample repeated for eight cycles at the strain above 200%.

Cycle	ε_n (%)	ε_m (%)	ε_u (%)	ε_p (%)	R_f (%)	R_r (%)
1st	0.450	216.2	215.9	10.45	99.86	95.36
2nd	10.45	219.4	219.1	10.94	99.86	99.77
3rd	10.94	215.5	215.3	11.17	99.90	99.89
4th	11.17	215.3	215.1	11.39	99.90	99.89
5th	11.39	215.2	214.9	11.57	99.85	99.91
6th	11.57	214.9	214.7	11.77	99.90	99.90
7th	11.77	214.8	214.5	11.94	99.85	99.92
8th	11.94	215.3	215.0	12.10	99.87	99.92

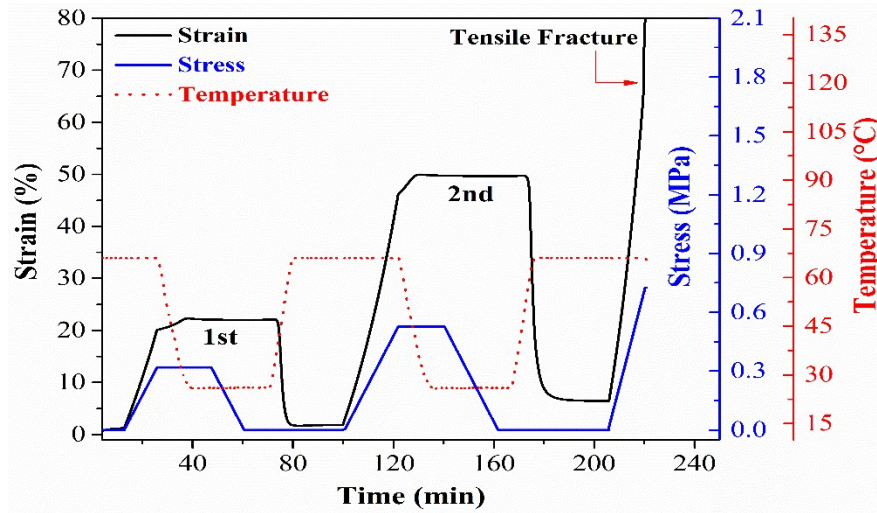


Figure S13. Shape memory cycle performance of CP-SMP sample at $T_d = T_r = T_g$ and $T_f = T_g - 40\text{ }^\circ\text{C}$ as the increasing of the strain (1st: $R_f = 100.0\%$, $R_r = 97.2\%$; 2nd: $R_f = 99.8\%$, $R_r = 90.3\%$).

Section S7. Stress relaxation isothermal tests:

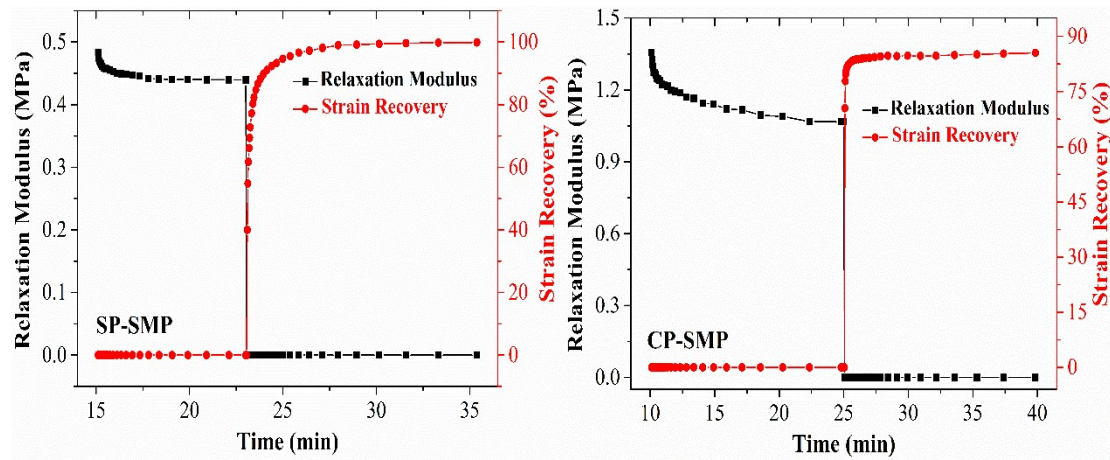


Figure S14. Stress relaxation and recovery of SP-SMP and CP-SMP at 1% strain at T_g .

Section S8. The multi-shape memory characterization:

Table S5 A comparison of the triple shape memory performance of SM-PN with representatively reported SMPs

Polymer systems	$R_f(\mathbf{A} \rightarrow \mathbf{B})$	$R_f(\mathbf{B} \rightarrow \mathbf{C})$	$R_f(\mathbf{C} \rightarrow \mathbf{B})$	$R_f(\mathbf{B} \rightarrow \mathbf{A})$	Ref
SM-PN	86.7%	99.1%	100.0%	100.0%	In the work
Bilayer epoxy	76.4%	96.4%	91.5%	98.5%	32
Bilayer polyurethane	80%	85%	–	85% $R_f(\mathbf{C} \rightarrow \mathbf{A})$	33
Epoxy/PCL composites	98.7%	74.4%	89.8%	91.5%	34
AB-polymer network	63.0%	99.1%	96.0%	101.6%	35
Side-chain liquid crystalline	74.8%	99.8%	98.0%	89.2%	36
Semi-interpenetrating polymer	55.4%	91.9%	85.0%	66%	23
SEBS/paraffin composites	65%	78%	99%	99%	37

Section S9. Multi-SME of semi-IPNs:

Fabrication of the representative P(MMA-co-MA)/PEG semi-IPNs: A representative semi-interpenetrating polymer network (semi-IPNs) was prepared by crosslinking of MA (4.3 g) and MMA (10 g) in the presence of 0.5 wt% AIBN, 0.5 wt% ethylene glycol dimethacrylate as a cross-linker and 20 wt% polyethylene glycol via radical polymerization. Nitrogen was bubbled through the reaction mixture for 15 min to remove any oxygen from the system, and the mixture was then injected into the space between two glass plates separated by silicone rubber spacers (1 mm thick). Polymerization was carried out at 55 °C for 24 h. All specimens were annealed at 120 °C for 30 min to ensure complete polymerization and then dried under a vacuum at 60 °C for 3 d to remove any unreacted monomer. Thermodynamics properties of SM-PN were characterized by DMA (Figure S15) and differential scanning calorimetry (DSC) (Figure S16).

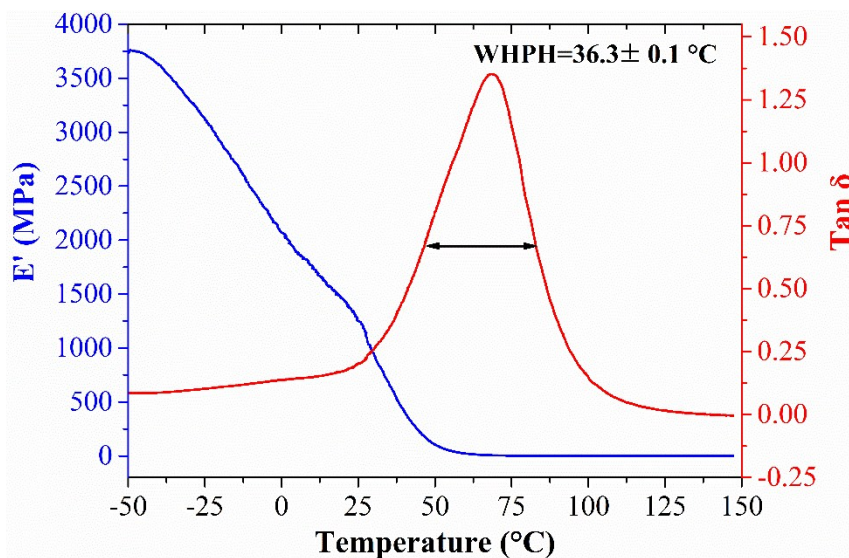


Figure S15. Storage modulus (E')-temperature and loss angle ($Tan \delta$)-temperature curves of the representative semi-IPNs ($T_g = 68.3 \pm 0.2 \text{ } ^\circ\text{C}$).

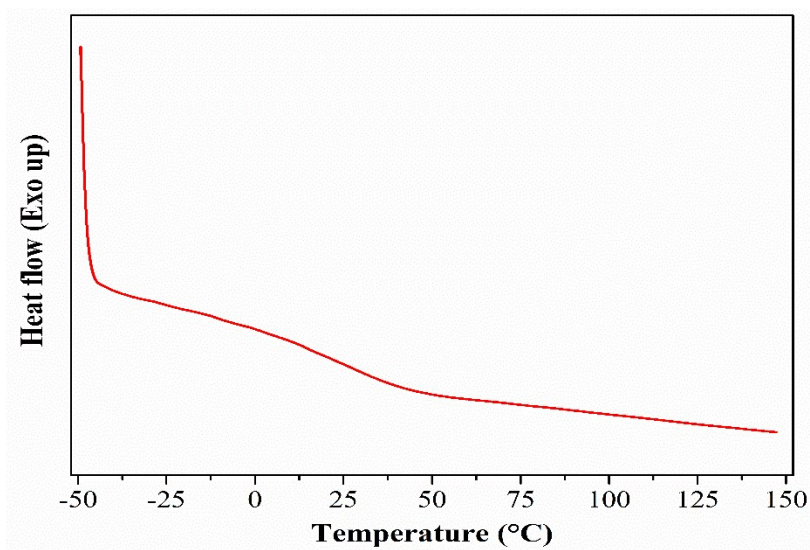


Figure S16. DSC thermogram (the second heating curve) of the representative semi-IPNs.

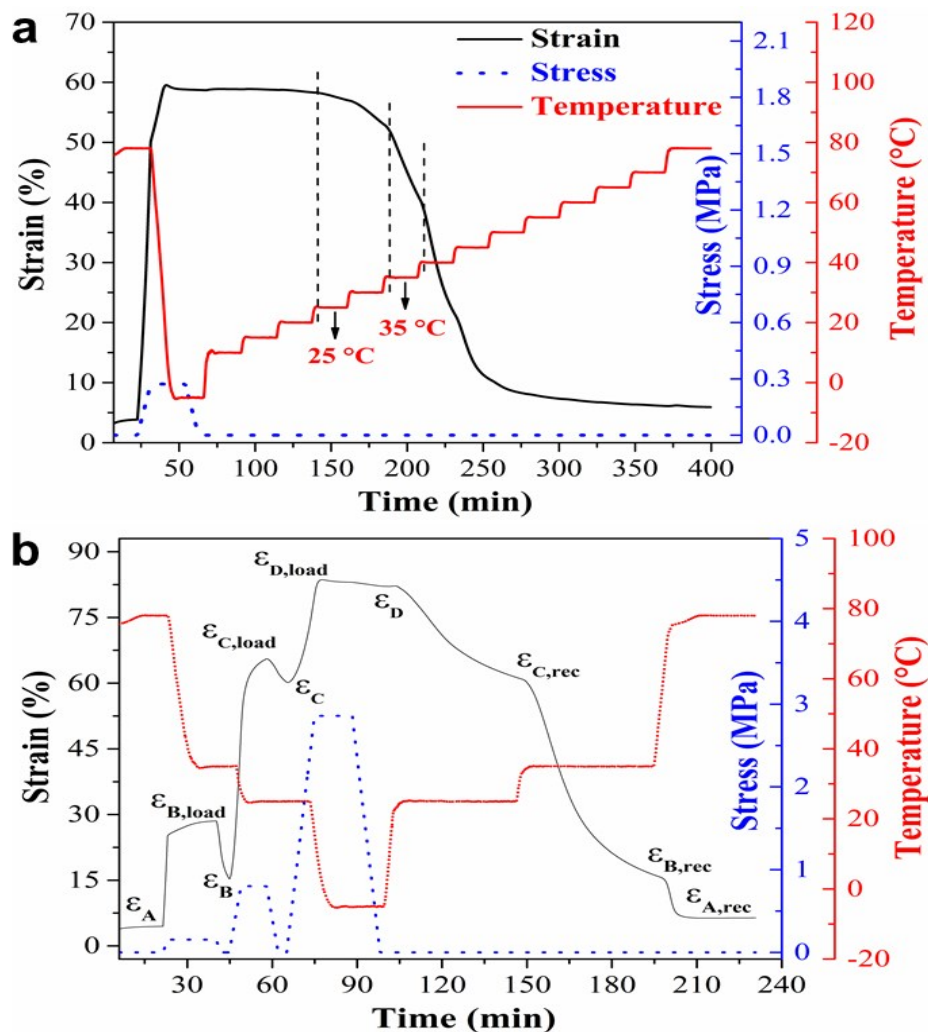


Figure S17. Tunable multi-SME of the representative P(MMA-co-MA)/PEG semi-IPNs. a) Multi-staged shape recovery at $T_d = 78 \text{ }^\circ\text{C}$, $T_f = -5 \text{ }^\circ\text{C}$ and multi-staged T_r from $10 \text{ }^\circ\text{C}$ to $78 \text{ }^\circ\text{C}$. b) Quadruple-SME with $T_{d1} = T_{r3} = 78 \text{ }^\circ\text{C}$, $T_{d2} = T_{f1} = T_{f2} = 35 \text{ }^\circ\text{C}$, $T_{d3} = T_{f2} = T_{f1} = 25 \text{ }^\circ\text{C}$ and $T_{f3} = -5 \text{ }^\circ\text{C}$. $R_r(\text{A} \rightarrow \text{B})$: 45.0%, $R_r(\text{B} \rightarrow \text{C})$: 89.4%, $R_r(\text{C} \rightarrow \text{D})$: 95.9%, $R_r(\text{D} \rightarrow \text{C})$: 96.7%, $R_r(\text{C} \rightarrow \text{B})$: 98.8%, $R_r(\text{B} \rightarrow \text{A})$: 82.3%.

Reference:

- 1 J. Xu, J. Song. High performance shape memory polymer networks based on rigid nanoparticle cores. *Proc. Natl. Acad. Sci. USA*, **2010**, 107, 7652-7654.
- 2 N. Y. Choi, A. Lendlein. Degradable shape-memory polymer networks from oligo[(L-lactide)-ran-glycolide]dimethacrylates. *Soft Matter*, **2007**, 3, 901-909.
- 3 P. T. Knight, K. M. Lee, T. Chung, P. T. Mather. PLGA-POSS end-linked

- networks with tailored degradation and shape memory behavior. *Macromolecules*, **2009**, 42, 6596-6605.
- 4 N. Y. Choi, S. Kelch, A. Lendlein. Synthesis, shape-memory functionality and hydrolytical degradation studies on polymer networks from poly(rac-lactide)-b-poly(propylene oxide)-b-poly(rac-lactide) dimethacrylates. *Adv. Eng. Mater.*, **2006**, 8, 439-445.
 - 5 S. Parker, R. Reit, H. Abitz, G. Ellson, K. Yang, B. Lund, W. E. Voit. High- T_g thiol-click thermoset networks via the thiol-maleimide michael addition. *Macromol. Rapid Commun.*, **2016**, 37, 1027-1032.
 - 6 A. Belmonte, D. Guzmán, X. Fernández-Francos, S. De la Flor. Effect of the network structure and programming temperature on the shape-memory response of thiol-epoxy “click” systems. *Polymers*, **2015**, 7, 2146-2164.
 - 7 O. D. McNair, B. J. Sparks, A. P. Janisse, D. P. Brent, D. L. Patton, D. A. Savin. Highly tunable thiol-ene networks via dual thiol addition. *Macromolecules*, **2013**, 46, 5614-5621.
 - 8 G. Ellson, M. Di Prima, T. Ware, X. Tang, W. Voit. Tunable thiol-epoxy shape memory polymer foams. *Smart Mater. Struct.*, **2015**, 24, 55001-55011.
 - 9 M. Podgórski, D. P. Nair, S. Chatani, G. Berg, C. N. Bowman. Programmable mechanically assisted geometric deformations of glassy two-stage reactive polymeric materials. *ACS Appl. Mater. Interfaces.*, **2014**, 6, 6111-6119.
 - 10 D. P. Nair, N. B. Cramer, T. F. Scott, C. N. Bowman, R. Shandas. Photopolymerized thiol-ene systems as shape memory polymers. *Polymer*, **2010**, 51, 4383-4389.
 - 11 M. Podgórski, E. Becka, S. Chatani, M. Claudino, C. N. Bowman. Ester-free thiol-X resins: new materials with enhanced mechanical behavior and solvent resistance. *Polym. Chem.*, **2015**, 6, 2234-2240.
 - 12 J. A. Carioscia, L. Schneidewind, C. O'Brien, R. Ely, C. Feeser, N. Cramer, C. N. Bowman. Thiol–norbornene materials: approaches to develop high T_g thiol–ene polymers. *J. Polym. Sci., Part A: Polym. Chem.*, **2007**, 45, 5686-5696.
 - 13 G. Zhang, Q. Zhao, W. Zou, Y. Luo, T. Xie. Unusual aspects of supramolecular

- networks: plasticity to elasticity, ultrasoft shape memory, and dynamic mechanical properties. *Adv. Funct. Mater.*, **2016**, 26, 931-937.
- 14 M. K. McBride, T. Gong, D. P. Nair, C. N. Bowman. Photo-mediated copper(I)-catalyzed azide-alkyne cycloaddition (CuAAC) “click” reactions for forming polymer networks as shape memory materials. *Polymer*, **2014**, 55, 5880-5884.
 - 15 M. Retailleau, A. Ibrahim, C. Croutxé-Barghorn, X. Allonas. New design of highly homogeneous photopolymer networks for shape memory materials. *RSC Adv.*, **2016**, 6, 47130-47133.
 - 16 K. Sunitha, K. S. S. Kumar, D. Mathew, C. P. R. Nair. Shape Memory Polymers (SMPs) derived from phenolic cross-linked epoxy resin via click chemistry. *Mater. Lett.*, **2013**, 99, 101-104.
 - 17 M. R. Ramdas, K. S. S. Kumar, C. P. R. Nair. Synthesis, structure and tunable shape memory properties of polytriazoles: dual-trigger temperature and repeatable shape recovery. *J. Mater. Chem. A*, **2015**, 3, 11596-11606.
 - 18 M. Ragin Ramdas, K. S. Santhosh Kumar, C. P. Reghunadhan Nair. Heat and solvent responsive polytriazole: shape recovery properties in different solvents. *RSC Adv.*, **2016**, 6, 53602-53613.
 - 19 S. Kelch, Nok. Y. Choi, Z. Wang, A. Lendlein. Amorphous, elastic AB copolymer networks from acrylates and poly[(L-lactide)-ran-glycolide]dimethacrylates. *Adv. Eng. Mater.*, **2008**, 10, 494-502.
 - 20 C. M. Yakacki, R. Shandas, C. Lanning, B. Rech, A. Eckstein, K. Gall. Unconstrained recovery characterization of shape-memory polymer networks for cardiovascular applications. *Biomaterials*, **2007**, 28, 2255-2263.
 - 21 D. Santiago, S. De la Flor, F. Ferrando, X. Ramis, M. Sangermano. Thermomechanical properties and shape-memory behavior of bisphenol A diacrylate-based shape-memory polymers. *Macromol. Chem. Phys.*, **2016**, 217, 39-50.
 - 22 Z. Li, Y. Pan, P. Zhang, Z. Zheng, X. Ding, Y. Peng, A novel shape memory polymer based on conetworks. *e-Polymers*, **2009**, 9, 295-302.
 - 23 J. Li, T. Liu, S. Xia, Y. Pan, Z. Zheng, X. Ding, Y. Peng. A versatile approach to

- achieve quintuple-shape memory effect by semi-interpenetrating polymer networks containing broadened glass transition and crystalline segments. *J. Mater. Chem.*, **2011**, 21, 12213-12217.
- 24 D. Ratna, J. Karger-Kocsis. Shape memory polymer system of semi-interpenetrating network structure composed of crosslinked poly (methyl methacrylate) and poly (ethylene oxide). *Polymer*, **2011**, 52, 1063-1070.
 - 25 G. Liu, C. Guan, H. Xia, F. Guo, X. Ding, Y. Peng. Novel shape-memory polymer based on hydrogen bonding. *Macromol. Rapid Commun.*, **2006**, 27, 1100-1104.
 - 26 X. Li, T. Liu, Y. Wang, Y. Pan, Z. Zheng, X. Ding, Y. Peng. Shape memory behavior and mechanism of poly (methyl methacrylate) polymer networks in the presence of star poly (ethylene glycol). *RSC Adv.*, **2014**, 4, 19273-19282.
 - 27 G. Liu, X. Ding, Y. Cao, Z. Zheng, Y. Peng. Novel shape-memory polymer with two transition temperatures. *Macromol. Rapid Commun.*, **2005**, 26, 649-652.
 - 28 S. Chen, F. Mo, Y. Yang, F. J. Stadler, S. Chen, H. Yang, Z. Ge. Development of zwitterionic polyurethanes with multi-shape memory effects and self-healing properties. *J. Mater. Chem. A*, **2015**, 3, 2924-2933.
 - 29 C. M. Yakacki, R. Shandas, D. Safranski, A. M. Ortega, K. Sassaman, K. Gall. Strong, tailored, biocompatible shape-memory polymer networks. *Adv. Funct. Mater.*, **2008**, 18, 2428-2435.
 - 30 T. Xie. Tunable polymer multi-shape memory effect. *Nature*, **2010**, 464, 267-270.
 - 31 Z. Yang, Y. Chen, Q. Wang, T. Wang. High performance multiple-shape memory behaviors of Poly(benzoxazole-co-imide)s. *Polymer*, **2016**, 88, 19-28.
 - 32 T. Xie, X. Xiao, Y. T. Cheng. Revealing triple-shape memory effect by polymer bilayers. *Macromol. Rapid Commun.*, **2009**, 30, 1823–1827.
 - 33 C. Y. Bae, J. H. Park, E. Y. Kim, Y. S. Kang, B. K. Kim. Organic–inorganic nanocomposite bilayers with triple shape memory effect. *J. Mater. Chem.*, **2011**, 21, 11288–11295.
 - 34 X. Luo, P. T. Mather. Triple-Shape Polymeric Composites (TSPCs). *Adv. Funct. Mater.*, **2010**, 20, 2649–2656.

- 35 I. Bellin, S. Kelch, R. Langer, A. Lendlein. Polymeric triple-shape materials. *Proc. Natl. Acad. Sci. USA*, **2006**, 103, 18043–18047.
- 36 S. K. Ahn, R. M. Kasi. Exploiting microphase-separated morphologies of side-chain liquid crystalline polymer networks for triple shape memory properties. *Adv. Funct. Mater.*, **2011**, 21, 4543–4549.
- 37 Q. Zhang, S. Song, J. Feng, P. Wu. A new strategy to prepare polymer composites with versatile shape memory properties. *J. Mater. Chem.*, **2012**, 22, 24776–24782.